International Journal of Advanced Engineering and Management Research

Vol. 11, No. 02; 2026

ISSN: 2456-3676

Experimental Study on the Effect of Concrete Cover Confinement on GFRP Bars Under Axial Compressive Loading

Phattaraphong Ponsorn
Department of Civil Engineering, Faculty of Engineering, Rajamangala University of Technology Krungthep, Bangkok 10120, Thailand
Corresponding author: phattaraphong.p@mail.rmutk.ac.th

doi.org/10.51505/ijaemr.2026.11235 URL: http://dx.doi.org/10.51505/ijaemr.2026.11235

Received: Apr 16, 2026 Accepted: Apr 21, 2026 Online Published: Apr 30, 2026

Abstract

Glass fiber reinforced polymer (GFRP) bars are increasingly used as reinforcement in concrete structures due to their corrosion resistance; however, limited experimental data exist on how concrete cover confinement influences the compressive behavior of GFRP bars, particularly when compared with conventional steel bars. This study experimentally investigates the effect of concrete cover confinement on the axial compressive capacity of GFRP bars. A total of 54 short column specimens were tested under axial compressive loading, including unconfined GFRP bars, unconfined steel bars, pure concrete specimens, and concrete-confined GFRP and steel bars. Three bar diameters, 10, 12, and 16 mm, were considered, with varying concrete cover diameters to evaluate the influence of the concrete cover area-to-bar area ratio. The test results indicate that concrete confinement significantly enhances the axial compressive capacity of GFRP bars, with the combined strength increasing as the concrete cover thickness increases. For all bar diameters, the ultimate load capacity of concrete-confined GFRP bars have a trend to exceed the simple summation of the capacities of the individual bar and pure concrete, demonstrating an effective confinement. Comparisons with steel bar specimens reveal that the confinement effect for GFRP bars is generally comparable, although slightly lower in the first and third sets of specimens. Overall, the experiment finds that concrete cover provides some beneficial confinement for GFRP bars under compression, and the effectiveness of this confinement is primarily governed by the ratio of concrete cover area to bar area. The results contribute to the compressive behavior of GFRP-reinforced concrete and provide useful experimental data for future analytical and design approaches.

Keywords: concrete cover confinement, GFRP bar, compressive strength, concrete confinement effect

1. Introduction

Glass fiber reinforced polymer (GFRP) bars have been increasingly adopted as an alternative to conventional steel reinforcement due to their corrosion resistance, high tensile strength, and

Vol. 11, No. 02; 2026

ISSN: 2456-3676

durability in aggressive environments. While the tensile behavior of GFRP-reinforced concrete members has been widely studied and addressed in design guidelines, the compressive performance of GFRP bars remains insufficiently understood. This limitation is primarily attributed to the brittle nature of GFRP bars, their relatively low elastic modulus, and premature failure mechanisms under compression, which raise concerns regarding their application in compression-dominant structural members such as columns and piles.

In reinforced concrete structures, reinforcing bars are embedded within concrete and benefit from lateral restraint provided by the surrounding material. Concrete cover confinement may therefore enhance the axial compressive capacity of GFRP bars by restraining local buckling and delaying failure. However, experimental evidence regarding the effectiveness of this confinement is still limited, and the influence of key parameters such as concrete cover thickness and bar diameter has not been clearly quantified. This study aims to experimentally investigate the effect of concrete cover confinement on the axial compressive strength of GFRP bars by testing concrete-confined and unconfined GFRP bars of various diameters, with comparative evaluation against steel bars and pure concrete specimens. The results provide insight into the confinement mechanism and contribute to improving the understanding and design of GFRP-reinforced concrete members under compression.

2. Literature Review

The use of fiber-reinforced polymer (FRP) reinforcement in concrete structures has gained increasing attention over the past several decades due to its corrosion resistance, high strength-to-weight ratio, and durability in aggressive environments. Among various FRP types, glass fiber–reinforced polymer (GFRP) bars are the most widely adopted because of their relatively low cost and ease of production. While extensive research has been conducted on the tensile behavior of GFRP-reinforced concrete members, leading to the inclusion of design provisions in several codes, the compressive behavior of GFRP bars and their contribution to axial load-bearing capacity remain less understood.

The beneficial role of confinement has been demonstrated in previous experiments; for example, An experiment (Ali et al., 2015) reported significant improvements in the axial capacity and deformation behavior of CFRP-wrapped reactive powder concrete columns. Later, experimental studies on isolated GFRP bars under axial compression reported that their compressive strength is significantly lower than their tensile strength, typically ranging between 30% and 60% of the tensile capacity (Abed et al., 2022; Benmokrane et al., 1995). Failure mechanisms were commonly associated with fiber micro-buckling, matrix cracking, and longitudinal splitting, resulting in brittle behavior without yielding (Bank, 2006; Jaitrong et al., 2025). Due to these characteristics and the limited available data, most design guidelines conservatively neglect or restrict the contribution of GFRP bars in compression members.

Later studies demonstrated that the compressive behavior of GFRP bars is strongly influenced by boundary conditions, test configuration, and lateral restraint (Khorramian & Sadeghian, 2021;

Vol. 11, No. 02; 2026

ISSN: 2456-3676

Zhou et al., 2023). Research (Zhou et al., 2023) showed that when appropriate test setups are adopted, GFRP bars exhibit stable linear elastic behavior up to failure, with relatively consistent compressive modulus values. Research (Khorramian & Sadeghian, 2021) further emphasized that the wide scatter in reported compressive strengths is largely attributable to non-standardized testing methods rather than inherent material variability.

When embedded in concrete, GFRP bars benefit from lateral restraint provided by the surrounding concrete, which can significantly enhance their compressive performance. Several experimental investigations on GFRP-reinforced concrete columns reported improved axial load capacity compared with unreinforced concrete members. Research (Afifi et al., 2014; Tobbi et al., 2014) observed that GFRP longitudinal reinforcement contributed positively to the axial strength of short concrete columns, despite its lower modulus of elasticity compared with steel reinforcement. Alsuhaibani et al. (Alsuhaibani et al., 2024) reported comparable axial capacities for GFRP- and steel-reinforced concrete columns when adequate confinement was present.

Concrete confinement is well known to enhance compressive strength and deformation capacity. Numerous studies on FRP-confined concrete columns demonstrated significant improvements in axial load capacity and ultimate strain due to confinement effects. Lam and Teng (Lam & Teng, 2003) and Teng et al. (Teng et al., 2007) established fundamental stress–strain relationships for FRP-confined concrete, while Valasaki and Papakonstantinou (Valasaki & Papakonstantinou, 2023) compiled a large experimental database confirming the effectiveness of FRP confinement for increasing compressive strength.

Only a limited number of studies have focused directly on the confinement effect of concrete on embedded FRP bars under compression. Lu et al. (Lu et al., 2023) investigated FRP-confined concrete-core-encased rebars and reported pronounced improvements in axial capacity and post-peak behavior compared with unconfined bars. Their results emphasized the importance of confinement stiffness and area ratio. Similarly, Li et al. (Li et al., 2016) showed that the axial resistance of concrete-filled FRP tubes increases with increasing confinement stiffness, suggesting that thicker concrete cover may improve bar stability.

Comparative studies between steel and GFRP bars under compression indicate that while steel reinforcement generally provides higher intrinsic compressive strength, GFRP bars exhibit similar confinement efficiency trends when adequately restrained. However, some researchers reported slightly reduced confinement effectiveness for GFRP bars due to their lower elastic modulus and absence of yielding behavior (AlNajmi & Abed, 2020).

Overall, the literature confirms that GFRP bars possess measurable compressive capacity and that concrete confinement can significantly enhance their axial performance. Nevertheless, systematic studies isolating the confinement effect of concrete cover, particularly as a function of concrete cover area-to-bar area ratio, remain limited. This clear research gap motivates the present experimental investigation.

Vol. 11, No. 02; 2026

ISSN: 2456-3676

3. Specimen Design, Preparation and Methodology

3.1 Specimen Design and Preparation

This experimental study aims to investigate the effect of concrete cover confinement on GFRP bars. The specimen geometry is illustrated in Figure 1, showing a typical configuration for a 10 mm diameter GFRP bar with a 100 mm diameter concrete cover. A total of 54 specimens were divided into three set categories, as shown in Table 1: the first set comprised 10 mm diameter GFRP bars (Specimens 1–18), while the second and third sets consisted of 12 mm (Specimens 19–36) and 16 mm diameter GFRP bars (Specimens 37–54), respectively. The first set comprised specimens with measured concrete cover diameters of 30.0, 51.1, 80.5, and 100.5 mm. While the second and third were 37.7, 65.3, 100.5, 125.0 and 44.3, 80.5, 128.4, 155.2 mm, respectively. The specimen heights for the first, second, and third sets were 50, 60, and 80 mm, respectively, maintaining a constant GFRP bar slenderness ratio, $\frac{Kl}{r}$, of 10 across all specimens.

PVC pipes (Polyvinyl chloride) were used as casting molds, as shown in Figure 2(a), and the three grouped set of GFRP and conventional steel bars were prepared as shown in Figure 2(b). After 28 days of concrete casting, all specimens were capped at both the top and bottom ends to ensure uniform load distribution during the compression tests using a universal testing machine (UTM).

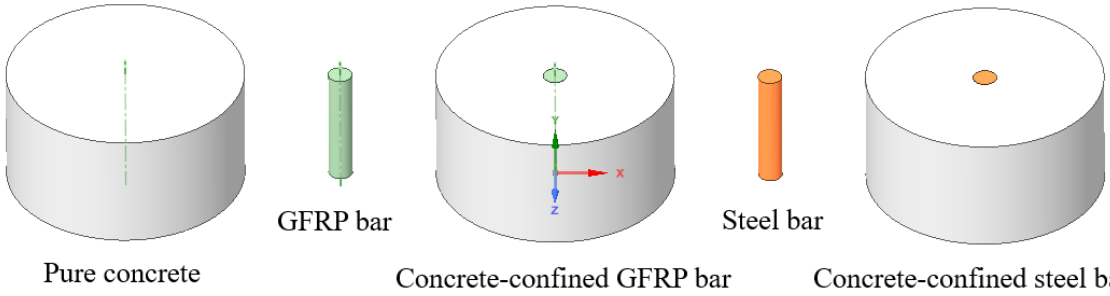

Figure 1. Geometric configuration of concrete cover confinement specimen (example of specimen GB10-C100).

Vol. 11, No. 02; 2026

ISSN: 2456-3676

(a) (b)

Figure 2. Specimen: (a) PVC cases and (b) GFRP and steel bars.

Table 1. Specimen dimensions and details.

No	Specimen	Description	L, mm	d_{bar}, mm	A_{bar}, mm^2	$d_{concrete}$, mm	$A_{net\ concrete}$, mm^2
1	C25	Pure concrete	50	0	0.00	30.0	706.86
2	C50	Pure concrete	50	0	0.00	51.1	2050.84
3	C75	Pure concrete	50	0	0.00	80.5	5089.58
4	C100	Pure concrete	50	0	0.00	100.5	7932.72
5	GB10-A	GFRP bar	50	10	78.54	-	-
6	GB10-B	GFRP bar	50	10	78.54	-	-
7	GB10-C	GFRP bar	50	10	78.54	-	-
8	GB10-C25	Concrete-confined GFRP bar	50	10	78.54	30.0	628.32
9	GB10-C50	Concrete-confined GFRP bar	50	10	78.54	51.1	1972.30
10	GB10-C75	Concrete-confined GFRP bar	50	10	78.54	80.5	5011.04
11	GB10-C100	Concrete-confined GFRP bar	50	10	78.54	100.5	7854.18
12	SB10-A	Steel bar	50	10	78.54	-	-
13	SB10-B	Steel bar	50	10	78.54	-	-
14	SB10-C	Steel bar	50	10	78.54	-	-
15	SB10-C25	Concrete-confined steel bar	50	10	78.54	30.0	628.32

Vol. 11, No. 02; 2026

ISSN: 2456-3676

16	SB10-C50	Concrete-confined steel bar	50	10	78.54	51.1	1972.30
17	SB10-C75	Concrete-confined steel bar	50	10	78.54	80.5	5011.04
18	SB10-C100	Concrete-confined steel bar	50	10	78.54	100.5	7854.18
19	C30	Pure concrete	60	0	0.00	37.7	1116.28
20	C60	Pure concrete	60	0	0.00	65.3	3349.01
21	C90	Pure concrete	60	0	0.00	100.5	7932.72
22	C120	Pure concrete	60	0	0.00	125.0	12271.85
23	GB12-A	GFRP bar	60	12	113.10	-	-
24	GB12-B	GFRP bar	60	12	113.10	-	-
25	GB12-C	GFRP bar	60	12	113.10	-	-
26	GB12-C30	Concrete-confined GFRP bar	60	12	113.10	37.7	1003.18
27	GB12-C60	Concrete-confined GFRP bar	60	12	113.10	65.3	3235.91
28	GB12-C90	Concrete-confined GFRP bar	60	12	113.10	100.5	7819.62
29	GB12-C120	Concrete-confined GFRP bar	60	12	113.10	125.0	12158.75
30	SB12-A	Steel bar	60	12	113.10	-	-
31	SB12-B	Steel bar	60	12	113.10	-	-
32	SB12-C	Steel bar	60	12	113.10	-	-
33	SB12-C30	Concrete-confined steel bar	60	12	113.10	37.7	1003.18
34	SB12-C60	Concrete-confined steel bar	60	12	113.10	65.3	3235.91
35	SB12-C90	Concrete-confined steel bar	60	12	113.10	100.5	7819.62
36	SB12-C120	Concrete-confined steel bar	60	12	113.10	125.0	12158.75
37	C40	Pure concrete	80	0	0.00	44.3	1537.86
38	C80	Pure concrete	80	0	0.00	80.5	5089.58
39	C120	Pure concrete	80	0	0.00	128.4	12948.51
40	C160	Pure concrete	80	0	0.00	155.2	18917.92
41	GB16-A	GFRP bar	80	16	201.06	-	-
42	GB16-B	GFRP bar	80	16	201.06	-	-
43	GB16-C	GFRP bar	80	16	201.06	-	-
44	GB16-C40	Concrete-confined	80	16	201.06	44.3	1336.80

Vol. 11, No. 02; 2026

ISSN: 2456-3676

45	GB16-C80	GFRP bar Concrete-confined GFRP bar	80	16	201.06	80.5	4888.51
46	GB16-C120	Concrete-confined GFRP bar	80	16	201.06	128.4	12747.45
47	GB16-C160	Concrete-confined GFRP bar	80	16	201.06	155.2	18716.86
48	SB16-A	Steel bar	80	16	201.06	-	-
49	SB16-B	Steel bar	80	16	201.06	-	-
50	SB16-C	Steel bar	80	16	201.06	-	-
51	SB16-C40	Concrete-confined steel bar	80	16	201.06	44.3	1336.80
52	SB16-C80	Concrete-confined steel bar	80	16	201.06	80.5	4888.51
53	SB16-C120	Concrete-confined steel bar	80	16	201.06	128.4	12747.45
54	SB16-C160	Concrete-confined steel bar	80	16	201.06	155.2	18716.86

3.2 Test Setup and Methodology

Axial compression tests were conducted using a calibrated hydraulic testing machine. All specimens were loaded concentrically under displacement-controlled conditions to ensure stable and uniform loading. The axial load was applied continuously until complete failure occurred. For each specimen, the ultimate compressive load and corresponding failure mode were recorded. Failure patterns were visually inspected and documented to identify governing mechanisms such as concrete crushing, bar buckling, splitting, or combined failure modes. The axial compressive capacities obtained from the confined specimens were compared with those of pure concrete and unconfined bars to evaluate the confinement effect. The confinement efficiency was quantified by assessing whether the combined capacity exceeded the summation of the individual contributions of concrete and reinforcement.

4. Results and Discussion

Following the failure tests of the three sets of specimens, the effect of concrete cover confinement on the axial compressive strength of GFRP bars is illustrated as clustered column chart in Figure 3. Figure 3(a) depicts the results for the first set of 10 mm diameter GFRP bars; the average compressive strength of the unconfined GFRP bars was 12.67 kN, which increased to a total combined capacity of 19, 63, 210, and 390 kN when embedded within concrete cover diameters of 30.0, 51.1, 80.5, and 100.5 mm, respectively. For comparison, the average compressive strength of the unconfined steel bars was 40.67 kN, which increased to a total of 38, 82, 227, and 403 kN when confined with the same concrete cover diameters. The pure concrete strengths for these same concrete cover diameters, regardless of the area replaced by the bars,

Vol. 11, No. 02; 2026

ISSN: 2456-3676

were 17, 51, 138, and 362 kN, respectively. The failures of the tested specimens are shown in Figure 4(a) and (d).

For second set of 12 mm diameter bars, the average compressive strength of the unconfined GFRP bars was 19.67 kN, as shown in Figure 3(b), which increased to a total combined capacity of 25, 79, 278 and 588 kN when embedded within concrete cover diameters of 37.7, 65.3, 100.5, and 125.0 mm, respectively. While the average compressive strength of the unconfined steel bars was 75 kN, which increased to a total of 74, 134, 351, and 602 kN when confined with the same concrete cover diameters. The pure concrete strengths for the same concrete cover diameters were 10, 67, 229, and 527 kN, respectively. The failures of the tested specimens are shown in Figure 4(b) and (e).

For the third set of 16 mm diameter bars, Figure 3(c) shows that the average compressive strength of the unconfined GFRP bars was 67.00 kN, which increased to a total combined capacity of 39, 125, 540 and 799 kN when embedded within concrete cover diameters of 44.25, 80.5, 128.4, and 155.2 mm, respectively. While the average compressive strength of the unconfined steel bars was 133.33 kN, which increased to a total of 52, 132, 545.33 and 884.33 kN when confined with the same concrete cover diameters. The pure concrete strengths for the same concrete cover diameters were 27, 102, 496, and 764 kN, respectively. The failures of the tested specimens are shown in Figure 4(c) and (f).

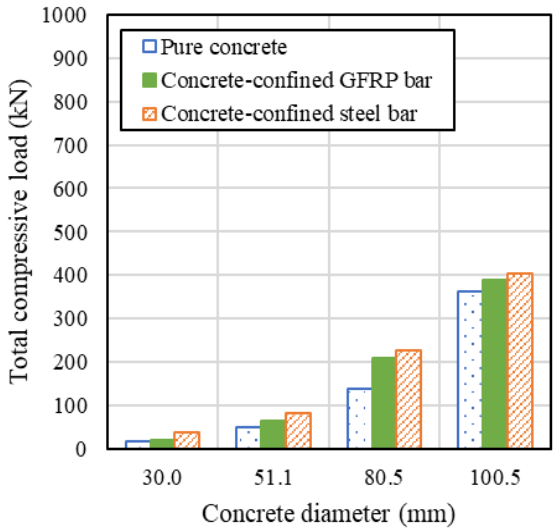

(a)

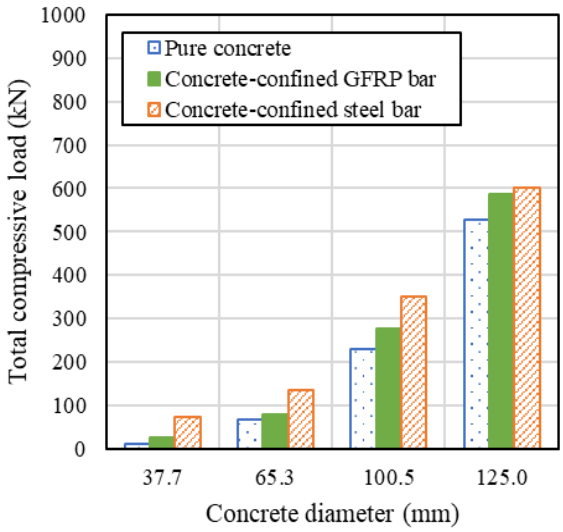

(b)

Vol. 11, No. 02; 2026

ISSN: 2456-3676

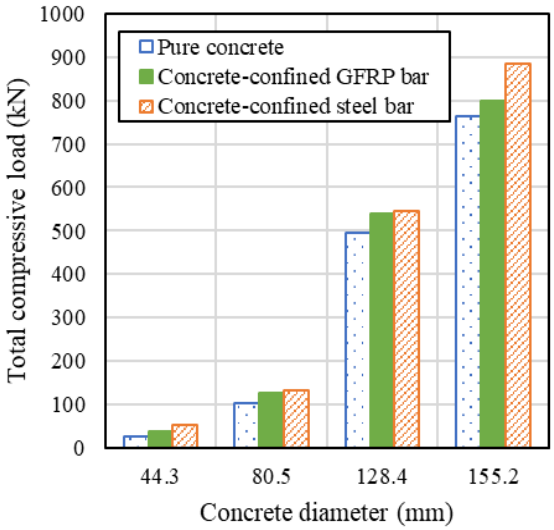

(c)

Figure 3. Results of axial compressive strength: (a) 10 mm diameter bar set, (b) 12 mm diameter bar set and (c) 16 mm diameter bar set.

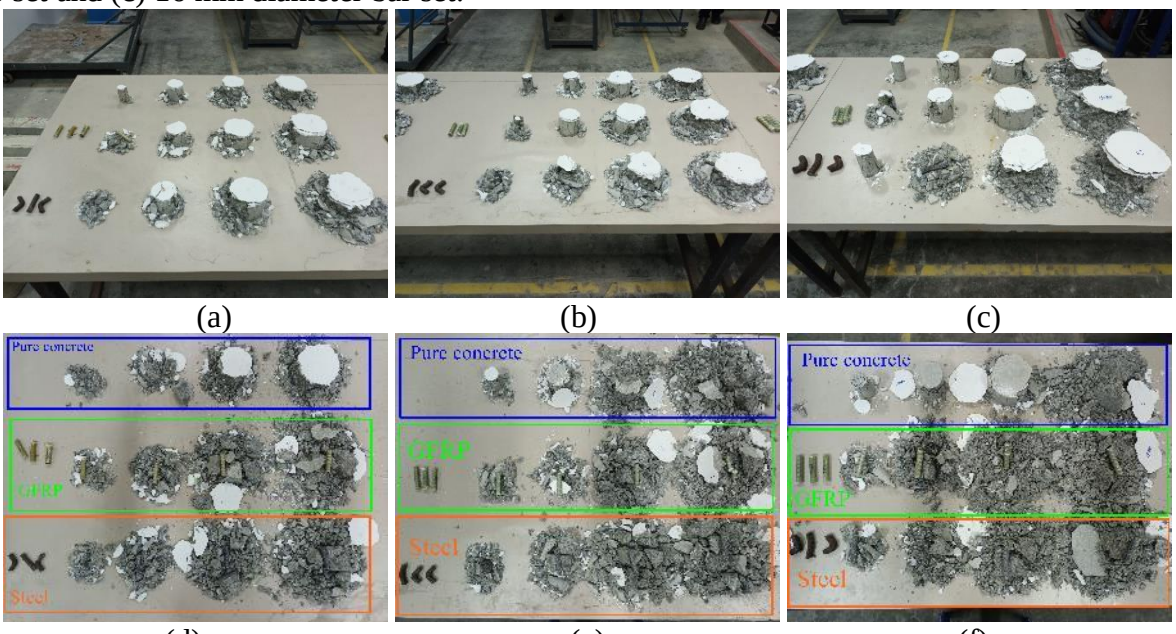

(a) (b) (c)

(d) (e) (f)

Figure 4. Failure of tested specimens: (a–c) general views of 10 mm, 12 mm, and 16 mm diameter bar sets; (d–f) investigation for 10 mm, 12 mm, and 16 mm diameter bars.

Vol. 11, No. 02; 2026

ISSN: 2456-3676

However, to distinctly investigate the effect of concrete cover confinement, which is expected to result in an axial capacity exceeding the simple sum of the individual GFRP bar and concrete strengths, the confinement effect is analyzed as follows:

$$\text{Concrete confinement increase} = \frac{P_{u,combined}}{P_{u,pure\ concrete} + P_{u,pure\ bar}} \quad (1)$$

where $P_{u,combined}$ is the ultimate axial compressive load for total combination of GFRP and steel bars, $P_{u,pure\ concrete}$ is the ultimate axial compressive load for pure concrete and $P_{u,pure\ bar}$ is the ultimate axial compressive load for pure GFRP and steel bars. Based on Equation (1), the calculated effects of concrete cover confinement against the ratio of concrete cover area to bar area are presented in Figure 5. The overall trend reveals that as the concrete cover area increases, the effectiveness of the confinement also increases, albeit slightly. The confinement effect is generally similar for both GFRP and conventional steel bars as shown in Figure 5(b); however, the 10 mm and 16 mm diameter specimens (shown in Figure 5(a) and Figure 5(c), respectively) exhibited a slightly lower confinement increase effect for the GFRP bars compared to the steel counterparts. Nevertheless, further studies should be conducted to investigate additional parameters, such as larger concrete cover areas, variations in concrete strength, other GFRP bar diameters, and the slenderness ratio of the specimens.

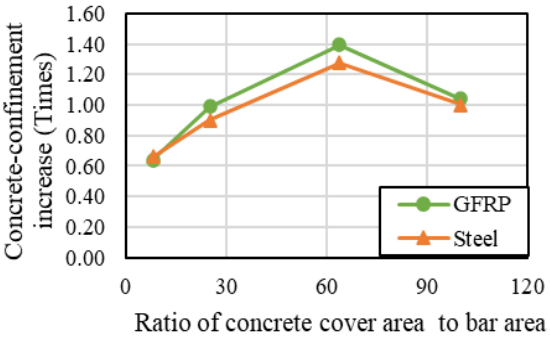

(a)

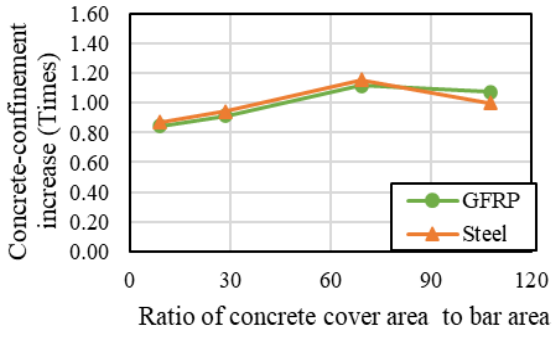

(b)

Vol. 11, No. 02; 2026

ISSN: 2456-3676

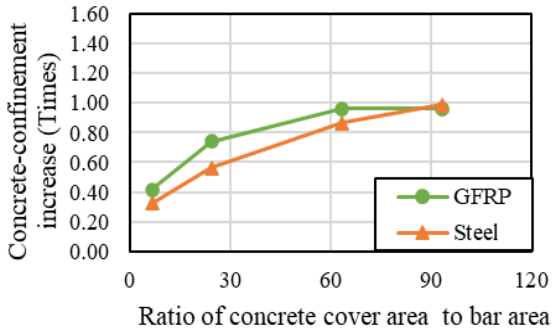

(c)

Figure 5. Effect of concrete cover confinement: (a) 10 mm diameter bar set, (b) 12 mm diameter bar set and (c) 16 mm diameter bar set.

5. Conclusion

This study experimentally investigated the effect of concrete cover confinement on the axial compressive behavior of GFRP bars through testing of 54 short specimens incorporating different bar diameters and concrete cover sizes. The results demonstrated that unconfined GFRP bars possess relatively low axial compressive capacity compared with conventional steel bars. However, when embedded within concrete cover, the compressive capacity of GFRP bars increased, albeit slightly, indicating that the surrounding concrete provides some lateral restraint and contributes to improved load resistance.

The experimental findings revealed that the combined axial compressive capacity of concrete-confined GFRP bars tend to exceed the simple summation of the capacities of pure concrete and the unconfined GFRP bar, confirming the presence of a confinement interaction effect. This confinement effect increased with the ratio of concrete cover area to bar area and was comparable to that observed in concrete-confined steel bars, although lower in some cases. Overall, the results confirm that concrete cover confinement has a trend of some beneficial role in enhancing the compressive performance of GFRP bars when embedded in concrete members, suggesting that GFRP reinforcement can be considered for compression concrete members when adequate confinement is provided. Further research is recommended to investigate the influence of additional parameters such as concrete strength, specimen slenderness, and larger confinement levels to support future design applications.

Declaration of Completing Interest

The author declares that they have no known competing financial interests of personal relationships that could have appeared to influence the work reported in this paper.

Vol. 11, No. 02; 2026

ISSN: 2456-3676

Data Availability

The data that support the findings of this study are available from the corresponding author upon reasonable request.

Acknowledgments

The author thanks Mr. Narat Ropru and Miss Nonpiya Sudsanguan for the laboratory assistance.

References

Abed, F., El Refai, A., & ElMesalami, N. (2022). Compressive behaviour of glass fiber-reinforced polymer (GFRP) reinforced concrete columns. In A. Ilki, M. Ispir, & P. Inci, Ilki, A., Ispir, M., Inci, P. (eds) 10th International Conference on FRP Composites in Civil Engineering. CICE 2021., Lecture Notes in Civil Engineering, vol 198. Springer, Cham.

Afifi, M. Z., Mohamed, H. M., & Benmokrane, B. (2014). Axial capacity of circular concrete columns reinforced with GFRP bars and spirals. *Journal of Composites for Construction*, *18*(1), 1-11. https://doi.org/doi:10.1061/(ASCE)CC.1943-5614.0000438

Ali, T. K. M., Ridha, M. M. S., Asaad, Z., & Yaseen, L. A. G. (2015). Comparison study of axial behavior of RPC-CFRP short columns. *Journal of Materials and Engineering Structures*, *2*(2), 57-67.

AlNajmi, L., & Abed, F. (2020). Evaluation of FRP bars under compression and their performance in RC columns. *Materials*, *13*(20), 4541.

Alsuhaibani, E., Alturki, M., Alogla, S. M., Alawad, O., Alkharisi, M. K., Bayoumi, E., & Aldukail, A. (2024). Compressive and bonding performance of GFRP-reinforced concrete columns. *Buildings*, *14*(4), 1071.

Bank, L. C. (2006). *Composites for construction: structural design with FRP materials*. John Wiley & Sons, Inc.

Benmokrane, B., Chaallal, O., & Masmoudi, R. (1995). Glass fibre reinforced plastic (GFRP) rebars for concrete structures. *Construction and Building Materials*, *9*(6), 353-364. https://doi.org/10.1016/0950-0618(95)00048-8

Jaitrong, J., Sirimontree, S., & Thongchom, C. (2025). Axial compression behavior of square concrete columns reinforced with longitudinal and transverse GFRP bars. *Results in Engineering*, *26*, 105032. https://doi.org/https://doi.org/10.1016/j.rineng.2025.105032

Khorramian, K., & Sadeghian, P. (2021). Material characterization of GFRP bars in compression using a new test method. *Journal of Testing and Evaluation*, *49*(2), 1037-1052. https://doi.org/10.1520/jte20180873

Lam, L., & Teng, J. G. (2003). Design-oriented stress–strain model for FRP-confined concrete. *Construction and Building Materials*, *17*(6), 471-489. https://doi.org/10.1016/S0950-0618(03)00045-X

Li, Y. L., Zhao, X. L., Singh, R. K. R., & Al-Saadi, S. (2016). Experimental study on seawater and sea sand concrete filled GFRP and stainless steel tubular stub columns. *Thin-Walled Structures*, *106*, 390-406. https://doi.org/10.1016/j.tws.2016.05.014

Lu, J., Huang, H., Li, Y., & Mou, T. (2023). Experimental and numerical investigation of axial

compression behaviour of FRP-confined concrete-core-encased rebar. *Polymers*, *15*(4), 1-16.

Teng, J. G., Huang, Y. L., Lam, L., & Ye, L. P. (2007). Theoretical model for fiber-reinforced polymer-confined concrete. *Journal of Composites for Construction*, *11*(2), 201-210. https://doi.org/doi:10.1061/(ASCE)1090-0268(2007)11:2(201)

Tobbi, H., Farghaly, A. S., & Benmokrane, B. (2014). Behavior of concentrically loaded fiber-reinforced polymer reinforced concrete columns with varying reinforcement types and ratios. *ACI structural journal*, *111*(2), 375-386. https://doi.org/10.14359/51686528

Valasaki, M. K., & Papakonstantinou, C. G. (2023). Fiber reinforced polymer (FRP) confined circular concrete columns: an experimental overview. *Buildings*, *13*(5), 1-57.

Zhou, Z., Meng, L., Zeng, F., Guan, S., Sun, J., & Tafsirojjaman, T. (2023). Experimental study and discrete analysis of compressive properties of glass fiber-reinforced polymer (gfrp) bars. *Polymers*, *15*(12), 2651.